Biophysical Journal Volume 101 October 2011 1968–1977

Mechanical Unfolding of Cardiac Myosin Binding Protein-C by Atomic Force Microscopy

Árpád Karsai,[†] Miklós S. Z. Kellermayer,[‡] and Samantha P. Harris[†*]
[†]University of California-Davis, Davis, California; and [‡]Semmelweis University, Budapest, Hungary

ABSTRACT Cardiac myosin-binding protein-C (cMyBP-C) is a thick-filament-associated protein that performs regulatory and structural roles within cardiac sarcomeres. It is a member of the immunoglobulin (Ig) superfamily of proteins consisting of eight Ig- and three fibronectin (FNIII)-like domains, along with a unique regulatory sequence referred to as the M-domain, whose structure is unknown. Domains near the C-terminus of cMyBP-C bind tightly to myosin and mediate the association of cMyBP-C with thick (myosin-containing) filaments, whereas N-terminal domains, including the regulatory M-domain, bind reversibly to myosin S2 and/or actin. The ability of MyBP-C to bind to both myosin and actin raises the possibility that cMyBP-C cross-links myosin molecules within the thick filament and/or cross-links myosin and thin (actin-containing) filaments together. In either scenario, cMyBP-C could be under mechanical strain. However, the physical properties of cMyBP-C and its behavior under load are completely unknown. Here, we investigated the mechanical properties of recombinant baculovirus-expressed cMyBP-C using atomic force microscopy to assess the stability of individual cMyBP-C molecules in response to stretch. Force-extension curves showed the presence of long extensible segment(s) that became stretched before the unfolding of individual Ig and FNIII domains, which were evident as sawtooth peaks in force spectra. The forces required to unfold the Ig/FNIII domains at a stretch rate of 500 nm/s increased monotonically from ~30 to ~150 pN, suggesting a mechanical hierarchy among the different Ig/FNIII domains. Additional experiments using smaller recombinant proteins showed that the regulatory M-domain lacks significant secondary or tertiary structure and is likely an intrinsically disordered region of cMyBP-C. Together, these data indicate that cMyBP-C exhibits complex mechanical behavior under load and contains multiple domains with distinct mechanical properties.

INTRODUCTION

Myosin-binding protein-C (MyBP-C) is a thick-filament-associated protein that performs both structural and regulatory roles within vertebrate muscle sarcomeres. Three major isoforms of MyBP-C are expressed in cardiac and fast and slow skeletal muscles (1). Each is encoded by a distinct gene, but all belong to the immunoglobulin (Ig) superfamily of proteins, since they all share a similar structural organization consisting of a series of domains that bear homology to either Ig-like or fibronectin (FNIII)-like folds (2). There are 10 such domains numbered C1–C10 in the skeletal isoforms, whereas cardiac (c) MyBP-C contains one additional Ig domain at the N-terminus of the molecule referred to as C0 (Fig. 1). Of the three isoforms, cMyBP-C has received the most intensive study, because mutations in *MYBPC3*, the gene encoding cMyBP-C, are among the most prevalent causes of hypertrophic cardiomyopathy causing heart failure in millions of people worldwide (3,4). Under normal physiological conditions, cMyBP-C contributes to increased cardiac contractility in response to β-adrenergic stimuli (5,6). Despite its broad physiological significance, however, the mechanisms by which cMyBP-C affects contraction and the significance of its Ig-domain architecture to the function(s) of cMyBP-C are not well understood.

The primary binding sites that anchor MyBP-C to the thick filament are located near the C-terminus within domains C8–C10 (Fig. 1), which link MyBP-C both to the light meromyosin section of the myosin rod and to titin along the thick filament (7–9). A second myosin-binding site, within domains C1-M-C2 near the N-terminus of MyBP-C, links MyBP-C to the S2 subfragment of myosin (i.e., to the myosin hinge) (10). Because it is abolished after phosphorylation by protein kinase A, binding to myosin S2 is thought to contribute to the functional effects of cMyBP-C to increase cardiac contractility, e.g., by reversibly anchoring myosin heads to the thick filament and thereby accelerating cross-bridge kinetics upon their release (11). The M-domain also binds F-actin and binds to thin filaments in a phosphorylation-sensitive manner, suggesting that these interactions could also contribute to regulated contractile responses to β-adrenergic agonists (12).

The ability of cMyBP-C to bind to two distinct locations on myosin and/or to bind both actin and myosin simultaneously raises the possibility that cMyBP-C either cross-links myosin molecules together within a thick filament or that it can cross-link adjacent thick and thin filaments. In these scenarios, cMyBP-C could either restrict the motion of myosin heads on the thick filament or oppose the relative sliding of thick and thin filaments. At the same time, such motions would be expected to impose strain on cMyBP-C, thereby potentially making it well-positioned to function as a mechanosensor that transduces mechanical movement into signaling pathways (13,14). However, to date there have been no studies investigating the mechanical properties of cMyBP-C under load. The purpose of the experiments

Submitted June 17, 2011, and accepted for publication August 19, 2011.
*Correspondence: samharris@ucdavis.edu
Editor: Hideo Higuchi.

0006-3495/11/10/1968/10 $2.00
doi: 10.1016/j.bpj.2011.08.030

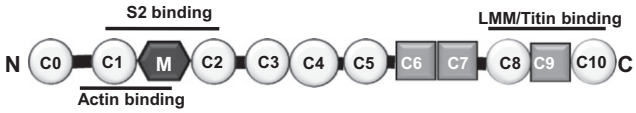

FIGURE 1 Schematic showing the domain structure of cMyBP-C. cMyBP-C is a modular protein composed of a series of 11 Ig- and FNIII-like domains numbered C0–C10 starting at the N-terminus of the protein. Ig-like domains are indicated by circles, FnIII-like domains are indicated by squares. A sequence rich in prolines and alanines (the P/A region) links domains C0 and C1. The regulatory M-domain is located between domains C1 and C2 and contains cardiac specific phosphorylation sites. Binding sites that anchor cMyBP-C to light meromyosin and titin of the thick filament are indicated by black lines near the C-terminus. Binding sites to myosin S2 and actin are indicated by black lines near the N-terminus of cMyBP-C.

discussed here was to use atomic force microscopy (AFM) to stretch individual cMyBP-C molecules and determine their behavior in response to applied force. The results demonstrate that the mechanical properties of cMyBP-C are heterogeneous, with Ig/FNIII-like domains unfolding over a range of relatively low forces (<150 pN) along with compliant regions, including the regulatory M-domain, that can be readily extended at forces <50 pN. The latter extensible segments may correspond to regions of poorly defined secondary or tertiary structure including intrinsically disordered regions. If so, then disorder-to-order transitions could confer functional plasticity to cMyBP-C during contraction or disease.

METHODS

Expression and purification of cMyBP-C proteins

Full-length murine cMyBP-C cDNA (Genbank accession number AF097333) was subcloned into a Topo XL vector (Invitrogen, Carlsbad, CA) after addition of BamH1 and Kpn1 sites to the 5′ and 3′ ends, respectively. For protein expression using a baculovirus system (Bac-to-Bac Baculovirus Expression System, Invitrogen), the BamH1/Kpn1 fragment was subcloned into the pFBacHTLA vector, and a Bacmid was made, propagated, and purified according to the manufacturer's protocol. Expression of cMyBP-C protein was confirmed by Western blot analysis of proteins produced from small-scale infections of adherent Sf9 cell cultures. The virus was then amplified and two rounds of plaque purification were performed. Large-scale virus cultures were made in Sf9 cell suspensions at low multiplicity of infection (MOI 0.20 pfu/cell). High-titer, low-passage viral stocks were stored at 4°C in the presence of 1% fetal calf serum.

For large-scale protein expression, Sf9 cells grown to log phase in suspension culture (0.6–1.2 L) in serum-free medium (SF900 III Medium, Invitrogen) were infected with cMyBP-C baculovirus at a MOI of 2 when cells reached ~2 million/ml. Cells were harvested 50–54 h postinfection, pelleted at 600 × *g*, and washed in cold phosphate-buffered saline (10 mM PO_4^- 150 mM NaCl, pH 7.2). Cell pellets were either used promptly or stored at −20°C. Partially thawed pellets were resuspended and lysed in ice-cold hypotonic Tris buffer (50 mM, pH 8.5) with protease inhibitors (0.375% EDTA-free Halt cocktail (Pierce Protein Research, Rockford, IL), three tablets of complete mini-EDTA-free protease inhibitor cocktail (Roche, Basel, Switzerland), 200 μM PMSF, 2.0 μg/ml pepstatin A, 10 μM phosphoramidon), 1% NP40 (detergent), and 2 mM β-mercaptoethanol (2-ME) for 1–2 h at 4°C with continuous rotation. cMyBP-C protein was purified from cell lysates by affinity purification using a cobalt resin (Talon resin, Clontech, Mountain View, CA) to bind a His_6-tag placed at the N-terminus of cMyBP-C. Protein bound to the column was washed in a low-imidazole loading buffer containing (in mM) 25 Tris, pH 8.5, 250 NaCl, 5 imidazole, 1.0 2-ME, and 0.1 EDTA and eluted with a gradient of imidazole from 5 mM to 250 mM. Peak fractions were pooled and dialyzed into K buffer containing (in mM) 300 KCl, 5.2 K2HPO4, 4.8 NaH2PO4, 2 NaN3, 0.1 EDTA, and 3 2-ME) for additional purification using a high-resolution hydroxylapatite column (Calbiochem, Gibbstown, NJ) according to Hartzell and Glass (15).

Recombinant mouse C1C2 was expressed and purified in *Escherichia coli* as described previously (12).

Protein preparation for atomic force microscopy

Immediately before use, purified proteins were clarified by ultracentrifugation at 400,000 × *g* for 20 min and diluted to 20–25 μg/ml in a buffer containing (in mmol/L) 20 MOPS, 100 KCl, pH 7.4, or in a cosedimentation buffer containing (in mmol/L) 20 imidazole, 180 KCl, 1 $MgCl_2$, 1 EGTA, 1 dithiothreitol, pH 7.4. Diluted proteins (~50 μl) were deposited by nonspecific adsorption onto cleaned glass slides or in some cases onto slides coated with Ni-NTA (Xenopore, London, United Kingdom) for adsorption via a His_6-tag at the N-terminus of cMyBP-C. After 10 min, unbound cMyBP-C was washed away by rinsing slides three times with fresh buffer (~100 μl).

AFM measurements

cMyBP-C molecules were mechanically stretched (Fig. 2) using an MFP3D atomic force microscope (Asylum Research, Santa Barbara, CA) and BioLever A cantilevers (Silicon nitride probe, gold-coated, Olympus, Melville, NY). The stiffness (*K*) of each cantilever was calibrated before use by measuring the thermally driven mean-square vertical bending of the cantilever tip and applying the equipartition theorem (16) using the built-in software of the AFM according to the equation

$$\frac{1}{2K\langle \Delta d^2 \rangle} = \frac{1}{2k_B T}, \tag{1}$$

where $<\Delta d^2>$ is the mean-square vertical cantilever bending, k_B is Boltzmann's constant, and T is the absolute temperature. Typical cantilever stiffness was ~30 pN/nm.

Force-versus-extension curves for individual cMyBP-C molecules were collected by pressing a cantilever tip to the protein-coated surface, then raising the cantilever tip up to stretch a cMyBP-C molecule adhered to the cantilever tip. The cantilever was raised up to 600 nm from the slide surface at constant pulling speeds (100, 500, 3000, or 5000 nm/s). Displacement of the cantilever base (s) was measured by using an integrated linear voltage differential transformer. Force (*F*) was obtained from cantilever bending (Δ*d*) according to

$$F = K\Delta d, \tag{2}$$

where *K* is the cantilever stiffness. Force-displacement curves were corrected to obtain force versus molecular end-to-end length according as follows. 1), The zero-length, zero-force data point was obtained from the force response that corresponded to the cantilever tip reaching (or departing from) the substrate surface. 2), Forces were corrected for baseline slope determined from the force response of unloaded cantilever. 3), The end-to-end length (*z*) of a tethered molecule was calculated by correcting the vertical displacement of the cantilever base with the bending of the cantilever:

$$z = s - \frac{F}{K}. \tag{3}$$

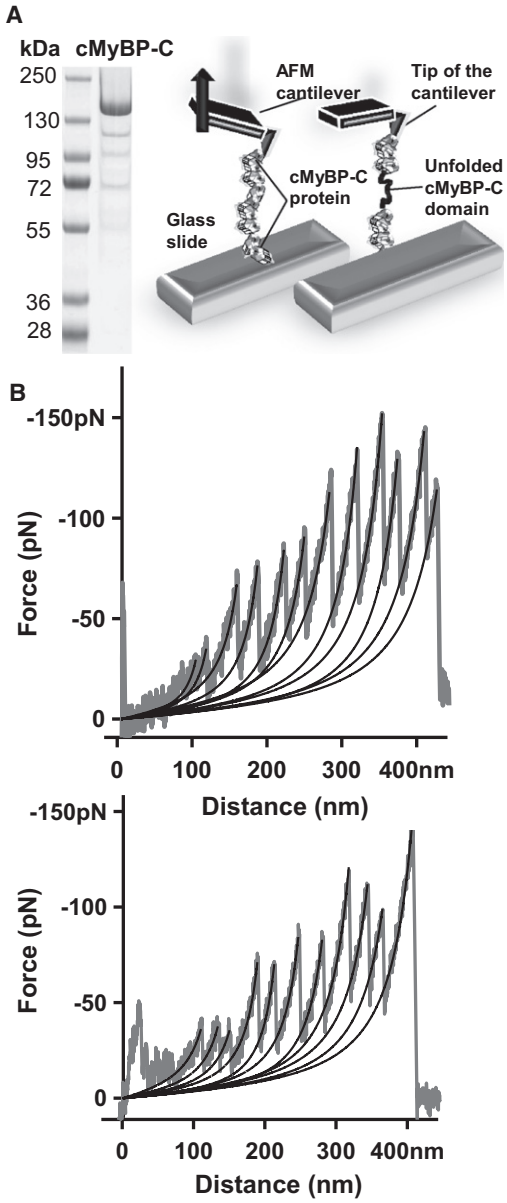

FIGURE 2 (*A*) Schematic of the experimental setup depicting the tip of an AFM cantilever stretching a single molecule of cMyBP-C. (*Inset*) Sodium dodecyl sulfate polyacrylamide gel electrophoresis of baculovirus-expressed cMyBP-C stained with Coomassie blue. (*B*) Two representative force-extension spectra obtained at a pulling speed of 500 nm/s. Stretching individual cMyBP-C molecules results in a pattern of sawtooth peaks indicative of Ig/FNIII domain unfolding. Black lines indicate WLC model fits to the data.

Contour-length (L_c) and persistence-length (L_p) values for the unfolded domains were obtained by fitting force data with the wormlike chain (WLC) equation (17):

$$\frac{FL_p}{k_BT} = \frac{Z}{L_C} + \frac{1}{4\left(\frac{1-Z}{L_C}\right)^2} - \frac{1}{4}. \quad (4)$$

Experiments were carried out at 299 ± 1 K. Experimental data curves were fit with the WLC equation using the built-in software of the Asylum AFM (Igor Pro 5.0, MFP version 050711, WaveMetrics, Lake Oswego, OR).

The unfolding force of individual domains was measured from the height of sawtooth peaks on the force-extension curves. Because force-extension curves often began with unusually high or irregular false peak(s) resulting from interactions between the cantilever tip and surface, peaks within ~50 nm of the zero-length point were usually excluded from analysis. The force peak accepted as corresponding to the first true unfolding event during a stretch was the one that featured a hyperbolic increase according to WLC behavior and ended with a sudden force drop followed by a sequence of similar (usually higher) peaks. The last peak in each spectrum was also excluded from force analysis due to detachment of the molecule from the cantilever tip (or from the surface). However, because extension before the final force peak/detachment event represents stretching of an adhered cMyBP-C molecule, extension distances before the final peak were included in calculations of total molecule contour length (L_c).

Statistics

Unless otherwise noted, all values represent mean ± SD.

RESULTS

Unfolding of cMyBP-C Ig- and FNIII-like domains

The mechanical stability of cMyBP-C was investigated by applying force to single cMyBP-C molecules using the cantilever tip of an AFM. Fig. 2 *A* shows a schematic for a typical experiment in which cMyBP-C proteins were randomly adhered to the tip of an AFM cantilever and stretched by moving the cantilever tip away from the slide surface. Two representative force-extension curves are shown in Fig. 2 *B*.

Stretching cMyBP-C resulted in a series of sawtooth force peaks characteristic of Ig- or FNIII-like domain unfolding, as previously described for other Ig-family proteins such as the giant muscle protein titin (18), and fibronectin (19). Most force-versus-extension curves were similar to those shown in Fig. 2 *B*, with regularly spaced sawtooth peaks corresponding to ordered unfolding events of individual Ig- or FNIII-like domains. However, other force curves were more irregular and jagged in appearance, with shorter spacing between the peaks. Jagged patterns were also reported for titin octamers consisting of eight identical titin Ig domains, where irregular spectra were explained as stretching of protein aggregates (doublets or multimers) instead of single molecules (20). To reduce the likelihood of including spectra resulting from simultaneous stretching of more than one molecule of cMyBP-C, we sorted force spectra into those with regular and those with irregular spacings and analyzed the groups separately. Although there were no significant differences in either the average contour length (32.2 ± 9.5 nm vs. 33.3 ± 15.4 nm for regular and irregular, respectively) or the mean unfolding force between the two groups 83.2 ± 30 pN vs. 79.3 ± 27 pN, respectively, at 500 nm/s pulling speed), irregular spectra were nevertheless excluded from summary data.

Out of 41 force-extension curves obtained at various pulling speeds, the maximum number of peaks in any one

spectrum was 11 (with the final, 12th peak representing detachment from the cantilever tip or from the slide surface), consistent with the predicted number of Ig- and FNIII-like domains within a single cMyBP-C molecule as deduced from primary amino acid sequence (2). In spectra with 11 peaks, the maximum measured contour length (L_c) was ~470 nm, in good agreement with the predicted L_c of 490 nm for the full-length murine cMyBP-C (0.38 nm/amino acid × 1289 amino acids). From these data, we conclude that force spectra containing 11 peaks correspond to the mechanical response of full-length cMyBP-C molecules.

Summary data from 20 partial and full-length force-extension curves with 6–11 sawtooth peaks (average molecular $L_c = 401 \pm 67$ nm) are shown in Fig. 3. The average L_c for the individual domains was 32.2 ± 9.5 nm, in agreement with theoretical lengths for the different domains between 30 and 49 nm (2). The average force required to unfold the domains was 83.2 ± 30 pN at a pulling speed of 500 nm/s. However, when plotted as a function of peak number, there was an orderly increase in unfolding force from ~40 pN required to unfold the first (lowest-stability) peak in a spectrum to >150 pN for the final peak (Fig. 3). The nearly threefold range in force required to unfold the first versus the last domain in a spectrum suggests that the different domains of cMyBP-C exhibit a wide range of mechanical stabilities. A similar wide range was reported for fibronectin (19), where unfolding forces increased from ~80 pN for the weakest domains to ~200 pN for the most stable domains. By contrast, only a 20% increase in force was required to unfold the first and last domains of a titin Ig octamer with eight identical domains of comparable stability (19–21).

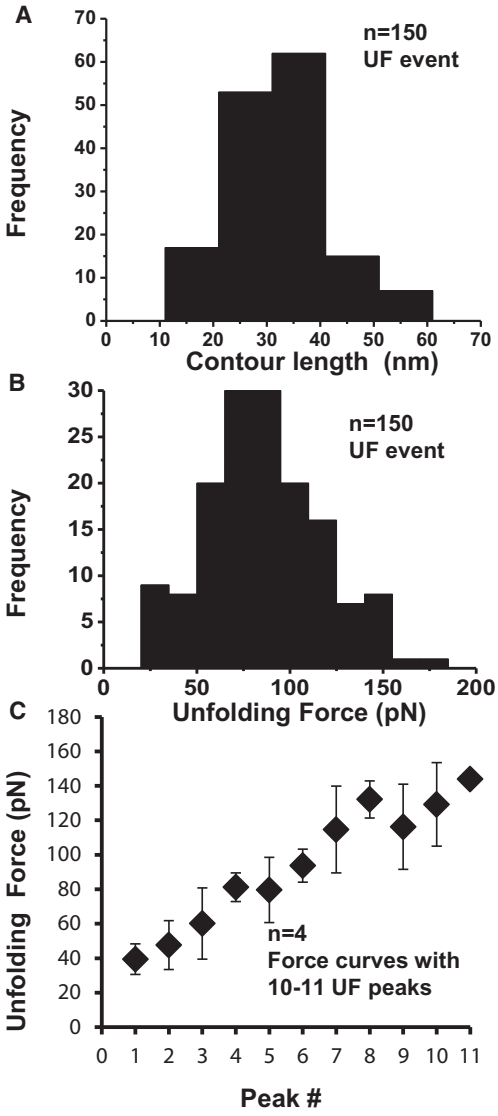

FIGURE 3 (*A*) Histogram showing the distribution of contour lengths (L_c) of individual Ig/FNIII domains. The average L_c (± SD) is 32.2 ± 9.5 nm. (*B*) Histogram showing the distribution of forces required to unfold individual Ig/FNIII domains. The average unfolding force is 83.2 ± 30 pN. (*C*) Plot of unfolding force versus peak position (peak number) in a force-extension spectrum. Increasing forces are required to unfold successive domains.

Rate dependence of unfolding forces and mechanical stability of different domains

Because force-extension curves suggested differences in the mechanical stability of the domains within cMyBP-C, we next probed for differences in domain behavior by measuring unfolding forces at various pulling speeds. Fig. 4 shows representative spectra and summary histograms of domain unfolding events at pulling speeds of 100, 500, 3000, and 5000 nm/s. At greater pulling speeds (3000 and 5000 nm/s), the average force required to unfold the domains shifted to higher values (106.7 ± 31.5 pN and 117.5 ± 39.3 pN, respectively) compared to values obtained at 500 nm/s (replotted from Fig. 3 for comparison), whereas at a lower pulling speed of 100 nm/s the average unfolding force was reduced to 59.8 ± 24.9 pN. These results correspond well to the expected exponential increase in unfolding force with increasing pulling speed as observed previously for titin Ig domains (18,22) and FNIII domains of fibronectin (19). However, whereas the histogram of unfolding force values at 500 nm/s pulling speed was well fitted with a single Gaussian distribution, at greater pulling speeds, the histogram distribution broadened such that at 5000 nm/s, two peaks became evident, one at ~102 pN and the second at ~151 pN. The spreading of the distribution suggests that the domains of cMyBP-C may be partitioned into two main populations according to their mechanical stability.

Structural coupling between domains

Although individual force-extension curves generally showed continuous increases in unfolding forces with each additional peak in the spectrum, we often observed instances where the unfolding force of a single peak would

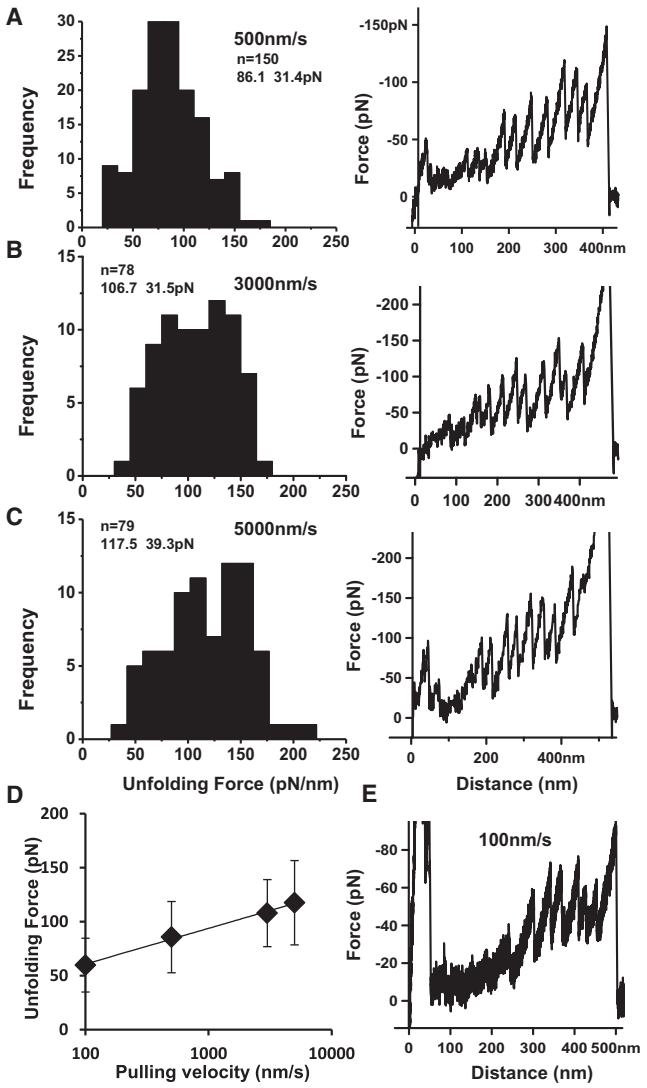

FIGURE 4 (*A–C*) Histograms showing the distribution of unfolding forces of Ig/FNIII domains measured at three different pulling speeds: 500 nm/s (data replotted from Fig. 3) (*A*), 3000 nm/s (*B*), and 5000 nm/s (*C*). Force-extension curves shown on the right are representative curves obtained at the corresponding pulling speed. (*D*) Average unfolding forces (± SD) obtained at each pulling speed, plotted as a function of pulling speed. Note the logarithmic increase in unfolding forces with pulling speed (*x* axis has a logarithmic scale). (*E*) Representative force extension curve obtained at 100 nm/s pulling velocity.

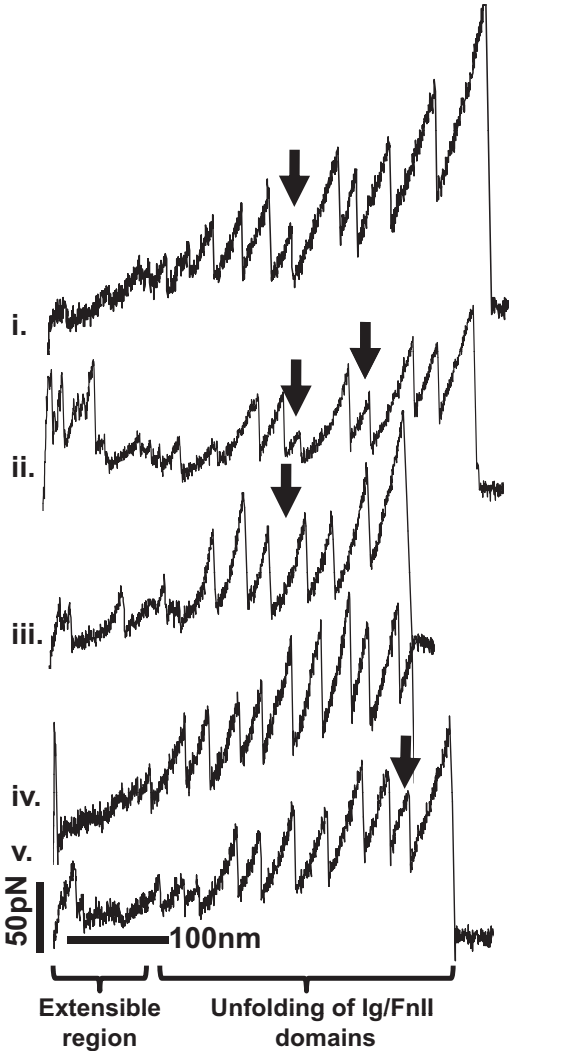

FIGURE 5 Common features of cMyBP-C force-extension curves. Gallery of five cMyBP-C force-extension curves illustrating characteristic features of the response of cMyBP-C to stretch. Arrows indicate anomalous force drops, where the unfolding of one domain occurs at a force lower than that of the domain preceding it. Brackets indicate the general division of spectra into a variable-length extensible segment that precedes the more regular unfolding of Ig/FNIII domains.

decrease before rising again with the next unfolding event, as shown in Fig. 5. These drops in force were unexpected, because unfolding of domains with lower stability should always precede unfolding of those with higher stability regardless of their sequential position in a tandem arrangement. However, the drops were frequent (e.g., in 17 of 23 spectra at 500 nm/s pulling speed) and were characterized by their appearance most frequently in the middle of the force spectrum. Typically, these occurred after around five to six unfolding events at forces >96.3 ± 18 pN, although they could also be observed earlier or later in the traces, e.g., after the first 2–4 unfolding peaks or before the ninth and tenth unfolding peaks. The magnitude of the force drops increased on average from 16.3 ± 6 pN to 28 ± 13.8 pN depending on whether they occurred early or late, respectively, in the spectra. Force drops were also observed at higher pulling speeds, where they occurred most commonly between peaks 5 and 8 or at forces >143 ± 11.7 pN, with an average magnitude drop of 38.4 ± 12 pN. Although the origin of the force drops is unknown at present, their frequency and reproducibility suggest that they correspond to specific structural features of cMyBP-C. One possibility is that some domains of cMyBP-C are mechanically coupled to one another such that unfolding of one domain leads to mechanical destabilization of an adjacent (or otherwise

coupled) domain. If so, then the force drops may be indicative of additional quaternary structural elements, arising, for instance, from interdomain interactions, such as between C5 and C8, and C7 and C10, as proposed for neighboring molecules (23), or from other intrinsic structural features of cMyBP-C. In support, electron microscope images demonstrated that cMyBP-C often adopts U- or V-shaped forms (24,25), and the bend in these images could represent coupled domains with distinct (lower or higher) flexibility.

Extensible and intrinsically disordered regions of cMyBP-C

In addition to the sawtooth force peaks that correspond to the unfolding of Ig- or FNIII-like domains of cMyBP-C, a long extensible segment was evident in most of the cMyBP-C force-extension spectra. The region was apparent as a long shallow rise in force that preceded unfolding of the first sawtooth peak such that the first unfolding event typically occurred at distances >100 nm from the surface (Figs. 2, 4, and 5). By fitting the first force peak with the WLC equation, an average contour length of 137.4 ± 25 nm was calculated for the extensible region (Fig. S1 in the Supporting Material). For full-length spectra, this distance is expected to include the contour length of the straightened cMyBP-C molecule or ~44 nm, as determined from electron microscope analyses of individual molecules (24,25). The remaining ~93 nm (137–44 nm) presumably represents compliant extension of other mechanically weak linkers or segments that are not integral to Ig/FNIII folding and/or other sequences that lack strong tertiary structure. The latter may include the 52-amino-acid linker sequence rich in proline and alanine residues (the P/A region) between domains C0 and C1, the structure of which is unknown but which has a theoretical L_c of ~20 nm (0.38 nm/amino acid), as well as the regulatory M-domain located between domains C1 and C2, which has a theoretical L_c of ~40 nm.

Previous small-angle x-ray scattering results suggested that the M-domain is compact and globular in solution, with overall dimensions similar to those of an Ig domain (26), but the absence of a 12th sawtooth peak in full-length AFM spectra, as well as NMR results by others (27), suggest that the M-domain lacks significant secondary or tertiary structure. To further investigate this possibility, we used a suite of computational algorithms in DisProt (28) to predict regions with a propensity for intrinsic disorder along the cMyBP-C sequence. Results from PONDR-FIT (29), VL3 (30,31), and VSL2B (32) algorithms are shown in Fig. 6. All three algorithms indicate that cMyBP-C contains multiple regions that are predicted to be intrinsically disordered, i.e., lacking in stable secondary or tertiary structure. Regions other than the M-domain and P/A region that are predicted to be disordered occurred throughout the length of cMyBP-C, most notably in sequences interconnecting

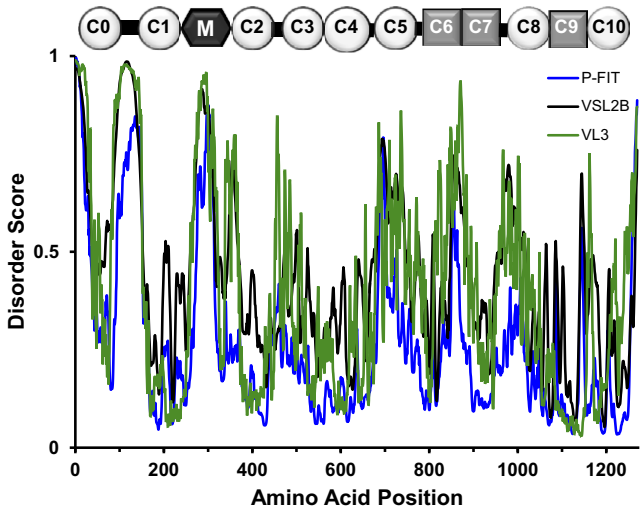

FIGURE 6 DisProt predictions of intrinsic disorder in cMyBP-C. Schematic diagram of cMyBP-C showing domain positions (approximations only) (*upper*) is aligned with scores from three disorder-prediction algorithms (PONDR-FIT, VSL2B, and VL3) plotted according to cMyBP-C residue number (*lower*). Scores >0.5 indicate a propensity toward disorder, whereas scores <0.5 indicate order. Approximate domain boundaries are C0, 8–95; C1, 151–253; C2, 356–434; C3, 448–542; C4, 553–611; C5, 641–761; C6, 768–860; C7, 865–958; C8, 967–1055; C9, 1062–1154; and C10, 1177–1265.

domains C2 and C3, C5 and C6, and C7 and C8. These disordered sequences could thus account for the remaining length of the extensible segment(s) measured in full-length AFM force-extension curves.

WLC fits of the extensible region in full-length force spectra yielded an average persistence length (L_p) of 0.65 ± 0.31 nm (Fig. S1). As shown by the histogram in Fig. S1, L_p values varied from 0.27 to 1.54 nm, with a well-defined peak at 0.42 nm. The higher L_p values and the wide range of values suggest that the disordered segments of cMyBP-C contain variable degrees of secondary structure, and that these may differ from molecule to molecule, as described for the wide distribution of L_p values for the PEVK domain of titin (33).

Mechanical properties of the M-domain

To further investigate the origins of the extensible segment(s) within cMyBP-C, and to determine whether the M-domain is compliant or whether it adopts a more stable folded conformation, we assessed the mechanical properties of a shorter recombinant construct, C1-M-C2 (i.e., C1C2), comprising the M-domain and its two flanking Ig domains, C1 and C2. Fig. 7 *A* shows representative force-extension curves obtained for C1C2 and summary data for 24 spectra obtained at a pulling speed of 1500 nm/s. The force-extension curves of C1C2 featured similar patterns that could be readily superimposed, indicating that the unfolding events were highly reproducible. The measured maximum

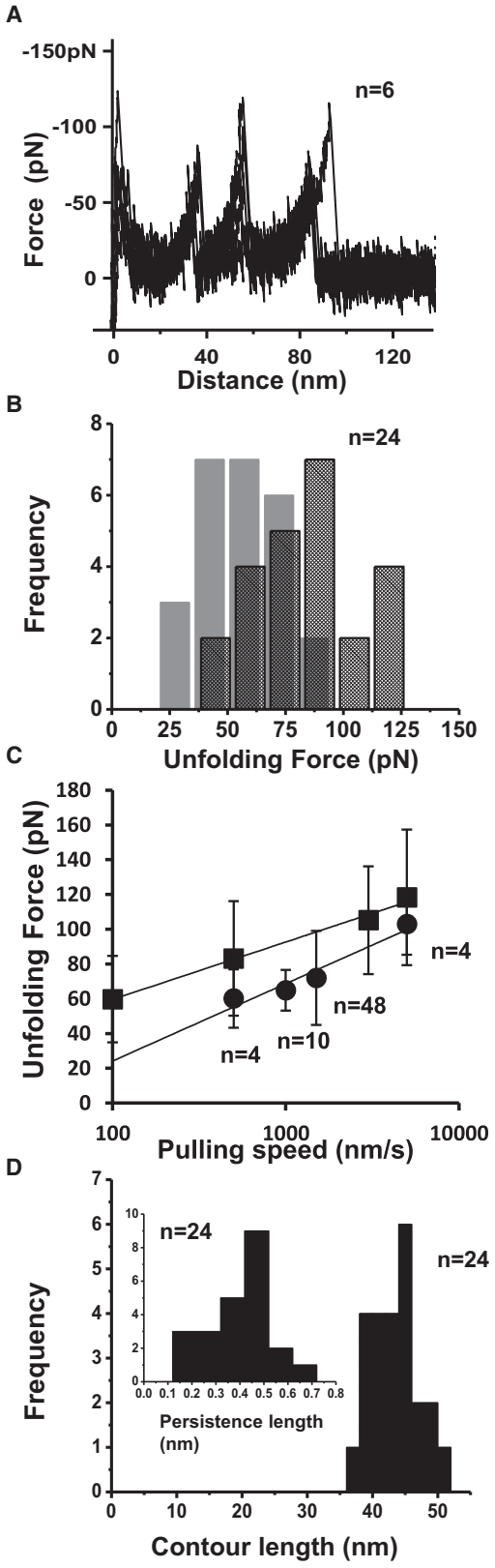

FIGURE 7 Force-extension spectra and summary data for C1C2. (*A*) Six individual force-extension spectra are shown superimposed to illustrate reproducibility of data. Individual spectra contained no more than two sawtooth peaks representing two Ig domain unfolding events, with a third (final) force peak indicating detachment from the cantilever or slide surface. (*B*) Histogram of unfolding force values for the first (*gray*) and second (*hatched*) sawtooth peaks in a spectrum. The average unfolding forces were 55.9 ± 17.3 pN and 84.6 ± 28.6 pN, respectively. (*C*) Pulling-speed dependence of unfolding forces for C1C2 (*circles*) compared to full-length cMyBP-C replotted from Fig. 4 (*squares*). (*D*) Histogram of L_c distributions for the extensible region preceding the first sawtooth peak. The average L_c was 43 ± 3.5 nm. (*Inset*) Histogram of L_p values for the extensible segment of C1C2. The average L_p value was 0.42 ± 0.14 nm.

L_c of C1C2 varied between 76.5 and 109 nm but did not exceed the theoretical maximum L_c for the full-length construct of 117 nm (309 amino acids × 0.38 nm/amino acid). The average L_c was 96.8 ± 9.9 nm, indicating that most spectra were slightly shorter than full length. The shorter-than-expected total contour length could have resulted if attachment of the construct to the surface prevented full mechanical access to the entire molecule. No more than two sawtooth peaks were seen in any one spectrum (i.e., no more than two peaks plus a detachment event). The two force peaks presumably correspond to the unfolding C1 and C2 with unfolding forces for the first and second peaks of 55.9 ± 17.3 and 84.6 ± 28.6 pN, respectively (Fig. 7 *B*). The pulling speed dependence for C1 and C2 unfolding is shown in Fig. 7 *C*.

A nonlinear elastic response before C1 and C2 unfolding events was observed which was qualitatively similar to that of the extensible region of the full-length cMyBP-C. As shown in Fig. 7 *D*, the L_c of the extensible segment varied between 37.6 and 50.5 nm, with an average of 43 ± 3.5 nm, in good agreement with the maximum theoretical L_c of the M-domain (~40 nm). However, since the L_c of the extensible region should also include the straightened length of the C1C2 molecule (~11 nm) (26), the true L_c of the M-domain is likely to be somewhat shorter, e.g., between ~32 and 43 nm. A shorter length suggests that even if the M-domain lacks overall stable folded tertiary structure, the M-domain may possess at least some secondary structural elements, such as α-helical segments that are not completely unfolded at low forces. However, because the average L_p of the extensible segment was 0.42 ± 0.14 nm (range 0.15–0.73 nm), comparable to the theoretical amino acid residue spacing of 0.38 nm, the M-domain is likely to be highly flexible and to adopt a compact conformation in the absence of imposed forces.

DISCUSSION

AFM experiments were carried out to determine the mechanical properties of individual cMyBP-C molecules in response to an applied force. Results establish a mechanical fingerprint for cMyBP-C and demonstrate that cMyBP-C comprises multiple heterogeneous segments with differing mechanical properties. Major conclusions from this study are that cMyBP-C is composed of a mixture

of stably folded Ig/FNIII-like domains along with extensible springlike regions, including the regulatory M-domain, that are likely to be intrinsically disordered. These properties could confer plasticity to the structure and function of cMyBP-C.

Low mechanical stability of cMyBP-C Ig/FNIII domains

The general appearance of cMyBP-C force-extension spectra are similar to other Ig/FNIII family proteins in that the most prominent features are the regular sawtooth peak patterns indicative of Ig/FNIII domain unfolding. However, cMyBP-C Ig/FNIII domains unfold at relatively low applied forces between 40 and 150 pN, whereas greater forces (~100–300 pN) are typically required to unfold domains of the giant muscle protein titin (34) or myomesin (35). In general, FNIII domains have lower stability than Ig domains and unfold between 100 and 200 pN compared to a range of 150–300 pN for Ig domains. Although cMyBP-C contains three FNIII-like domains (C6, C7, and C9), the data presented here cannot distinguish whether the FNIII domains of cMyBP-C are of lower stability than the Ig domains. For instance, data from the C1C2 construct suggest that the N-terminal Ig C1 and C2 domains may belong to the low-stability category, because the first unfolding event in C1C2 force-extension spectra occurs at forces of 55.9 ± 17.3 pN (Fig. 7). However, the stability of C1 and C2 in the truncated C1C2 protein may be reduced relative to the native protein due to surface interactions or the absence of flanking domains (e.g., C0 and C3), since individual FNIII domains appear more stable in the native protein compared to when they were expressed separately in a tandem FNIII-Ig27 octamer (19).

The relatively low forces required to unfold cMyBP-C Ig/FNIII domains and the wide range of stabilities is similar to that of fibronectin, which consists of tandem FNIII domains that unfold with forces ranging from 80 to 200 pN (19). It was suggested that fibronectin's ability to unfold at relatively low forces could facilitate a role for it as a mechanosensor, since moderate forces could reveal cryptic binding sites for matrix assembly or signaling molecules similar to mechanical modulation of the kinase domain of titin (14). The prevalence of low-stability domains and extensible segments within cMyBP-C suggests that it, too, could be well suited to serving mechanosensing functions. It will thus be of interest to determine whether binding or activation of signaling molecules such as Ca^{2+}-calmodulin-dependent kinase that copurifies with cMyBP-C (15) are influenced by the mechanical load on cMyBP-C. In a similar way, it is an interesting possibility that ligand-binding sites such as those to actin (12) or myosin S2 (36) that occur within the extensible M-domain may be mechanically modulated and become cryptically exposed once cMyBP-C is stretched.

Unfolding of cMyBP-C in sarcomeres

Because the precise localization of cMyBP-C within the sarcomere and its binding partners are not fully known, the actual mechanical load imposed on cMyBP-C, and the behavior of cMyBP-C in response to stretch remain speculative. However, cMyBP-C is anchored to the thick filament by binding of domains C8–C10 at its C-terminus to the myosin rod and to A-band titin (8,9). Domains C8–C10 are thus likely protected from mechanical deformation in a manner similar to stabilization of titin's Z1Z2 domains by telethonin (37) or titin's A-band domains by the myosin thick filament. On the other hand, N-terminal domains of cMyBP-C, especially C0–C2, undergo phosphorylation-dependent binding interactions with myosin S2, actin, and/or other thin-filament proteins in vitro (11,12). These segments or intervening regions between the N-terminal and C-terminal binding sites, such as domains C2–C7, could thus be subject to mechanical strain imposed by either the relative sliding of thick and thin filaments (Fig. S2) or the motion of the myosin heads and S2 hinge region during contraction. In either event, cMyBP-C could constitute an internal load that impedes cross-bridge motion (38,39). If so, then the low overall stability of cMyBP-C suggests that the magnitude of such a load may be somewhat modest, or that it would only be imposed after extensible slack is taken up by first stretching the molecule. This could account for observations that MyBP-C slows myocyte shortening velocities after ~85 nm of sarcomere shortening (38).

Intrinsically disordered segments of cMyBP-C

A characteristic feature of cMyBP-C force-extension curves was the presence of one or more segments that could be extended ~130 nm before the unfolding of Ig/FNIII domains. This length likely includes straightening of the full-length cMyBP-C molecule, as well as extension of any compliant sequences within cMyBP-C that lack stable secondary or tertiary structure. It should be noted that both the proline-alanine rich region linking the C0 and C1 domains and the regulatory M-domain are predicted to be intrinsically disordered (Fig. 6), consistent with NMR results by others (27) and AFM results presented here (Fig. 7) that support the idea that the M-domain lacks significant stable secondary or tertiary structure.

The finding that the M-domain is readily extensible at low applied forces, combined with the conclusion that the M-domain is compact in solution (26), suggests that it may behave as an elastic element, relaxing back into a globular conformation after release from stretch. If so, then the M-domain could act as an entropic spring similar to the PEVK domain of titin or the EH domain of myomesin (40). cMyBP-C could thus enhance relaxation rates, accounting in part for the slowed relaxation of hearts and myocytes from cMyBP-C knockout mice (41,42). An alternative

scenario is that the flexibility of the M-domain could increase its ability to interact with multiple binding partners, similar to p53, which leverages structural plasticity to create specific binding sites for >100 different binding partners (43). Flexibility might also augment the capture of target proteins at a distance (e.g., fly-casting mechanisms). Intrinsic disorder of the M-domain may thus explain its ability to bind multiple partners or to mediate low-affinity, high-specificity dynamic interactions that can be rapidly formed and yet readily dispersed, as for microtubule-associated proteins that dynamically cross-link microtubules but do not impede the sliding of filaments past one another (44).

The prediction of intrinsically disordered regions throughout cMyBP-C (Fig. 6) suggests that additional segments outside of the M-domain are also specialized for flexibility. A notable example is the proline-alanine-rich segment, which is predicted to be entirely disordered. Although the function of this segment is unknown, an inverse correlation between the percentage of proline and alanines and mammalian heart rate suggests that there might be some regulatory function under evolutionary pressure for selection (45). Strikingly, however, hypertrophic cardiomyopathy missense mutations have not been linked to the proline-alanine-rich region, suggesting that single amino acid substitutions do not disrupt its function or are otherwise well tolerated (4). One possibility is that the proline-alanine region functions as an entropic chain similar to the ball-and-chain inactivation mechanisms of voltage-gated potassium channels that use a mobile chain to set the time preceding channel inactivation by modulating the time it takes for a chained plug to search for and block the channel pore (46). Other entropic chains function as bristles or brushes to maintain neurofilament spacing (47).

Additional studies are needed to determine the precise functions of the different intrinsically disordered regions within cMyBP-C, but their presence suggests a new repertoire of regulatory mechanisms that can rapidly modulate the function of cMyBP-C, since disorder-to-order transitions are especially sensitive to factors such as protein phosphorylation state, pH, charge, ionic strength, and temperature (48,49). It is an intriguing possibility that dynamic changes in these variables, including changes in divalent ion concentrations, can produce dynamic changes in the mechanical properties of cMyBP-C or influence its binding interactions with target ligands within the time frame of a single heart beat.

SUPPORTING MATERIAL

Two figures are available at http://www.biophysj.org/biophysj/supplemental/S0006-3495(11)01003-4.

The authors thank Elaine Hoye for her expert technical assistance in protein expression and purification, Jeffrey Forbes for insights into protein intrinsic disorder, Attila Nagy for fruitful discussions and helpful comments on the manuscript, and Alan Hicklin for technical assistance in the University of California, Davis, Spectral Imaging Facility.

This work was supported by National Institutes of Health grant R01 HL080367 to S.P.H. and by a grant from the Hungarian Science Foundation (OTKA K73256) to M.S.Z.K.

REFERENCES

1. Yamamoto, K., and C. Moos. 1983. The C-proteins of rabbit red, white, and cardiac muscles. *J. Biol. Chem.* 258:8395–8401.
2. Carrier, L., G. Bonne, …, K. Schwartz. 1997. Organization and sequence of human cardiac myosin binding protein C gene (MYBPC3) and identification of mutations predicted to produce truncated proteins in familial hypertrophic cardiomyopathy. *Circ. Res.* 80:427–434.
3. Xu, Q., S. Dewey, …, A. V. Gomes. 2010. Malignant and benign mutations in familial cardiomyopathies: insights into mutations linked to complex cardiovascular phenotypes. *J. Mol. Cell. Cardiol.* 48:899–909.
4. Harris, S. P., R. G. Lyons, and K. L. Bezold. 2011. In the thick of it: HCM-causing mutations in myosin binding proteins of the thick filament. *Circ. Res.* 108:751–764.
5. Stelzer, J. E., J. R. Patel, and R. L. Moss. 2006. Protein kinase A-mediated acceleration of the stretch activation response in murine skinned myocardium is eliminated by ablation of cMyBP-C. *Circ. Res.* 99:884–890.
6. Tong, C. W., J. E. Stelzer, …, R. L. Moss. 2008. Acceleration of crossbridge kinetics by protein kinase A phosphorylation of cardiac myosin binding protein C modulates cardiac function. *Circ. Res.* 103:974–982.
7. Moos, C., G. Offer, …, P. Bennett. 1975. Interaction of C-protein with myosin, myosin rod and light meromyosin. *J. Mol. Biol.* 97:1–9.
8. Flashman, E., H. Watkins, and C. Redwood. 2007. Localization of the binding site of the C-terminal domain of cardiac myosin-binding protein-C on the myosin rod. *Biochem. J.* 401:97–102.
9. Gilbert, R., M. G. Kelly, …, D. A. Fischman. 1996. The carboxyl terminus of myosin binding protein C (MyBP-C, C-protein) specifies incorporation into the A-band of striated muscle. *J. Cell Sci.* 109:101–111.
10. Gautel, M., O. Zuffardi, …, S. Labeit. 1995. Phosphorylation switches specific for the cardiac isoform of myosin binding protein-C: a modulator of cardiac contraction? *EMBO J.* 14:1952–1960.
11. Gruen, M., H. Prinz, and M. Gautel. 1999. cAPK-phosphorylation controls the interaction of the regulatory domain of cardiac myosin binding protein C with myosin-S2 in an on-off fashion. *FEBS Lett.* 453:254–259.
12. Shaffer, J. F., R. W. Kensler, and S. P. Harris. 2009. The myosin-binding protein C motif binds to F-actin in a phosphorylation-sensitive manner. *J. Biol. Chem.* 284:12318–12327.
13. Lammerding, J., R. D. Kamm, and R. T. Lee. 2004. Mechanotransduction in cardiac myocytes. *Ann. N. Y. Acad. Sci.* 1015:53–70.
14. Gautel, M. 2011. Cytoskeletal protein kinases: titin and its relations in mechanosensing. *Pflugers Arch.* 462:119–134.
15. Hartzell, H. C., and D. B. Glass. 1984. Phosphorylation of purified cardiac muscle C-protein by purified cAMP-dependent and endogenous Ca^{2+}-calmodulin-dependent protein kinases. *J. Biol. Chem.* 259:15587–15596.
16. Hutter, J. L., and J. Bechhoefer. 1993. Calibration of atomic-force microscope tips. *Rev. Sci. Instrum.* 64:1868–1873.
17. Bustamante, C. 1994. Probing biological surfaces. *Science.* 264:296.
18. Rief, M., M. Gautel, …, H. E. Gaub. 1997. Reversible unfolding of individual titin immunoglobulin domains by AFM. *Science.* 276:1109–1112.
19. Oberhauser, A. F., C. Badilla-Fernandez, …, J. M. Fernandez. 2002. The mechanical hierarchies of fibronectin observed with single-molecule AFM. *J. Mol. Biol.* 319:433–447.
20. Watanabe, K., C. Muhle-Goll, …, H. Granzier. 2002. Different molecular mechanics displayed by titin's constitutively and differentially expressed tandem Ig segments. *J. Struct. Biol.* 137:248–258.

21. Carrion-Vazquez, M., P. E. Marszalek, …, J. M. Fernandez. 1999. Atomic force microscopy captures length phenotypes in single proteins. *Proc. Natl. Acad. Sci. USA.* 96:11288–11292.

22. Carrion-Vazquez, M., A. F. Oberhauser, …, J. M. Fernandez. 1999. Mechanical and chemical unfolding of a single protein: a comparison. *Proc. Natl. Acad. Sci. USA.* 96:3694–3699.

23. Moolman-Smook, J., E. Flashman, …, H. Watkins. 2002. Identification of novel interactions between domains of yosin binding protein-C that are modulated by hypertrophic cardiomyopathy missense mutations. *Circ. Res.* 91:704–711.

24. Hartzell, H. C., and W. S. Sale. 1985. Structure of C protein purified from cardiac muscle. *J. Cell Biol.* 100:208–215.

25. Swan, R. C., and D. A. Fischman. 1986. Electron microscopy of C-protein molecules from chicken skeletal muscle. *J. Muscle Res. Cell Motil.* 7:160–166.

26. Jeffries, C. M., A. E. Whitten, …, J. Trewhella. 2008. Small-angle X-ray scattering reveals the N-terminal domain organization of cardiac myosin binding protein C. *J. Mol. Biol.* 377:1186–1199.

27. Ababou, A., E. Rostkova, …, M. Pfuhl. 2008. Myosin binding protein C positioned to play a key role in regulation of muscle contraction: structure and interactions of domain C1. *J. Mol. Biol.* 384:615–630.

28. Sickmeier, M., J. A. Hamilton, …, A. K. Dunker. 2007. DisProt: the Database of Disordered Proteins. *Nucleic Acids Res.* 35(Database issue):D786–D793.

29. Xue, B., R. L. Dunbrack, …, V. N. Uversky. 2010. PONDR-FIT: a meta-predictor of intrinsically disordered amino acids. *Biochim. Biophys. Acta.* 1804:996–1010.

30. Obradovic, Z., K. Peng, …, A. K. Dunker. 2003. Predicting intrinsic disorder from amino acid sequence. *Proteins.* 53 (*Suppl 6*):566–572.

31. Peng, K., S. Vucetic, …, Z. Obradovic. 2005. Optimizing long intrinsic disorder predictors with protein evolutionary information. *J. Bioinform. Comput. Biol.* 3:35–60.

32. Peng, K., P. Radivojac, …, Z. Obradovic. 2006. Length-dependent prediction of protein intrinsic disorder. *BMC Bioinformatics.* 7:208.

33. Li, H., A. F. Oberhauser, …, J. M. Fernandez. 2001. Multiple conformations of PEVK proteins detected by single-molecule techniques. *Proc. Natl. Acad. Sci. USA.* 98:10682–10686.

34. Granzier, H., M. Helmes, …, K. Trombitas. 2000. Mechanical properties of titin isoforms. *Adv. Exp. Med. Biol.* 481:283–300, discussion 300–284.

35. Bertoncini, P., R. Schoenauer, …, H. J. Güntherodt. 2005. Study of the mechanical properties of myomesin proteins using dynamic force spectroscopy. *J. Mol. Biol.* 348:1127–1137.

36. Gruen, M., and M. Gautel. 1999. Mutations in β-myosin S2 that cause familial hypertrophic cardiomyopathy (FHC) abolish the interaction with the regulatory domain of myosin-binding protein-C. *J. Mol. Biol.* 286:933–949.

37. Bertz, M., M. Wilmanns, and M. Rief. 2009. The titin-telethonin complex is a directed, superstable molecular bond in the muscle Z-disk. *Proc. Natl. Acad. Sci. USA.* 106:13307–13310.

38. Hofmann, P. A., M. L. Greaser, and R. L. Moss. 1991. C-protein limits shortening velocity of rabbit skeletal muscle fibres at low levels of Ca^{2+} activation. *J. Physiol.* 439:701–715.

39. Palmer, B. M., T. Noguchi, …, M. M. LeWinter. 2004. Effect of cardiac myosin binding protein-C on mechanoenergetics in mouse myocardium. *Circ. Res.* 94:1615–1622.

40. Schoenauer, R., P. Bertoncini, …, I. Agarkova. 2005. Myomesin is a molecular spring with adaptable elasticity. *J. Mol. Biol.* 349:367–379.

41. Harris, S. P., C. R. Bartley, …, R. L. Moss. 2002. Hypertrophic cardiomyopathy in cardiac myosin binding protein-C knockout mice. *Circ. Res.* 90:594–601.

42. Pohlmann, L., I. Kröger, …, L. Carrier. 2007. Cardiac myosin-binding protein C is required for complete relaxation in intact myocytes. *Circ. Res.* 101:928–938.

43. Uversky, V. N., and A. K. Dunker. 2010. Understanding protein nonfolding. *Biochim. Biophys. Acta.* 1804:1231–1264.

44. Walczak, C. E., and S. L. Shaw. 2010. A MAP for bundling microtubules. *Cell.* 142:364–367.

45. Shaffer, J. F., and S. P. Harris. 2009. Species-specific differences in the Pro-Ala rich region of cardiac myosin binding protein-C. *J. Muscle Res. Cell Motil.* 30:303–306.

46. Hoshi, T., W. N. Zagotta, and R. W. Aldrich. 1990. Biophysical and molecular mechanisms of Shaker potassium channel inactivation. *Science.* 250:533–538.

47. Brown, H. G., and J. H. Hoh. 1997. Entropic exclusion by neurofilament sidearms: a mechanism for maintaining interfilament spacing. *Biochemistry.* 36:15035–15040.

48. Bright, J. N., T. B. Woolf, and J. H. Hoh. 2001. Predicting properties of intrinsically unstructured proteins. *Prog. Biophys. Mol. Biol.* 76:131–173.

49. Müller-Späth, S., A. Soranno, …, B. Schuler. 2010. From the Cover: Charge interactions can dominate the dimensions of intrinsically disordered proteins. *Proc. Natl. Acad. Sci. USA.* 107:14609–14614.